Review Article *Open Access*

Journal of Modern Classical Physics & Quantum Neuroscience

ISSN: 3068-4196

DOI: doi.org/10.63721/26JPQN0177

Scattering-Dominated Intermediate-Energy Neutron: An Analytical Ramsauer Model

Seyed Ali Rahbani

Department of Energy Engineering and Physics, Amirkabir University of Technology, Hafez Ave., Tehran, Iran

Citation: *Seyed Ali Rahbani (2026) Scattering-Dominated Intermediate-Energy Neutron: An Analytical Ramsauer Model. J.of Mod Phy & Quant Neuroscience 2(4), 1-9. WMJ/JPQN-177*

Abstract

This study presents a theoretically grounded approach for computing intermediate-energy neutron–nucleus cross sections using an analytically simplified Ramsauer model. Building on the optical model and employing the Wentzel–Kramers–Brillouin approximation, compact expressions for scattering, total, and reaction (removal) cross sections are derived under the assumption of an angular-momentum-independent complex phase shift. Calculations for representative light and heavy nuclides (^{12}C, ^{16}O, ^{107}Ag, and ^{235}U) are benchmarked against ENDF/B-VIII.0 data over 0.25–2 MeV.Relative error analysis indicates that the model reproduces the overall energy dependence of the scattering cross section, σ_sc, with mean deviations of 15–45%, while σ_r is systematically overestimated—most strongly for light nuclei where evaluated data indicate negligible absorption. For ^{235}U, the model preserves the correct energy trend but requires parameter tuning to match evaluated magnitudes.From an application standpoint, these findings are directly relevant to fast-spectrum and epithermal portions of Generation IV reactor systems (e.g., SFR/LFR/GFR), where intermediate-energy transport in structural materials, reflectors, and coolant/moderator constituents affects spectrum shaping, leakage, and reactivity feedback. If used without calibration, an overestimated removal term can bias neutron balance predictions, leading to conservative estimates of flux distributions and k_eff, and affecting computed reaction-rate ratios and material worth. In radiation shielding for fast reactors—such as vessel, reflector, and containment shielding, and streaming paths through penetrations-the same bias can produce overly conservative attenuation and shift predicted spectral hardening, influencing thickness optimization and dose/activation estimates.

***Corresponding author**: Seyed Ali Rahbani, Department of Energy Engineering and Physics, Amirkabir University of Technology, Hafez Ave., Tehran, Iran.

Submitted: 22.06.2026 **Accepted**: 26.06.2026 **Published**: 09.07.2026

Keywords: Endf/B-Viii.0 Comparison, Intermediate Neutron Energies, Neutron-Nucleus Cross Sections, Ramsauer Model, Relative Error Analysis, Wkb Approximation

Introduction

The neutron cross section is a fundamental parameter for characterizing neutron–matter interactions, particularly within nuclear reactor systems, where it plays a crucial role in accurately predicting neutron behavior [1,2]. Methods for determining neutron cross sections are generally categorized into three main approaches: experimental measurements, computational simulations, and theoretical modeling [1,3,4 5, 6, 7, 8, 9].

Historically, neutron cross-section data have been predominantly obtained through experimental measurements performed in specialized laboratories and subsequently compiled in comprehensive nuclear data libraries, such as the Evaluated Nuclear Data File (ENDF) [9]. Although experimental methods provide highly reliable results, they are often costly and require advanced facilities that may not be readily accessible to many academic and research institutions. Therefore, validating theoretical predictions against experimental benchmarks remains essential for refining nuclear reaction models and minimizing dependence on extensive experimental campaigns.

In theoretical studies, pioneering work on medium-energy neutron cross-section calculations was conducted by [10]. Foundational research in this field originated at the University of Cambridge in 1935 and has since evolved through contributions from numerous researchers and institutions. Over the decades, various theoretical approaches have been developed, each offering distinct levels of complexity and predictive accuracy [12]. Many of these models exhibit strong consistency with experimental data, particularly in the medium-energy range, thereby demonstrating their potential to complement or substitute experimental efforts [13,14,3,7]. Among these, the optical model represents a comparatively simple yet effective framework that employs a complex potential to estimate neutron cross sections [13]. The present study focuses on the analytical evaluation of neutron cross sections using the optical/Ramsauer model. The calculated results are compared with experimental data available in the ENDF database. While the optical model has traditionally been applied to high-energy neutron interactions, this work investigates its applicability within the less-explored intermediate-energy region.The remainder of this paper is organized as follows: Section 2 introduces the theoretical formulation and analytical framework; Section 3 presents the computed neutron cross sections for selected elements and compares them with experimental data; and Section 4 summarizes the main findings and outlines directions for future research.

A theoretically consistent Ramsauer model for neutron cross section based on the optical potential and WKB approximation

While the optical model offers a satisfactory explanation, its calculations involve numerous partial waves, which complicates the derivation of a straightforward or intuitive understanding of the underlying physical mechanisms. In contrast, the nuclear Ramsauer model [15] presents a more fundamental perspective, where the forward scattering amplitude for a neutron interacting with a nucleus is described by Equation. (1).

$$f(0^\circ) = \frac{i}{2k}\sum_{l=0}^{L}(2l+1)\left(1-e^{i\alpha\delta}\right) \tag{1}$$

In this context, the complex phase shift δ is assumed to be independent of the angular momentum quantum number [16]. Based on this assumption, and by summing over l up to a maximum value L= kR_{ch} [17, 18, 19], Equation. (1) simplifies to Equation. (2). The wave number k used in this expression is defined in Equation. (3).

$$f(0^\circ) = \frac{ik(R_{ch}+\lambda)^2}{2}\left(1-\alpha e^{i\beta}\right) \tag{2}$$

$$\lambda = \frac{1}{k} = \frac{\hbar}{\sqrt{2mE}} \tag{3}$$

Where, E is the incident neutron energy in the center-of-mass system, m is the reduced mass of the neutron-nucleus system, and Rch is the channel radius. The parameter β corresponds to twice the real part of the phase shift and governs the oscillatory behavior, while α describes attenuation due to absorption. From the partial wave analysis of scattering theory, we arrive at Eq. (4) and Eq. (5). Where, ηl is given by Equation. (6).

$$\sigma_{sc} = \frac{\pi}{k^2}\sum_{l=0}^{\infty}(2l+1)\,|1-\eta_l|^2 \tag{4}$$

The above expressions show that the total cross section can be expressed in terms of a small number of physically meaningful parameters, namely the channel radius, the real part of the phase shift, and the attenuation factor associated with absorption. This feature makes the model particularly suitable for studying systematics of neutron–nucleus interactions, since complex partial-wave dependent optical model calculations are avoided without losing the essential physics.

$$\sigma_r = \frac{\pi}{k^2}\sum_{l=0}^{\infty}(2l+1)\,|1-|\eta_l|^2| \tag{5}$$

$$\eta_l = e^{2i\delta_l} \tag{6}$$

Assuming that $\delta_l=\delta$ is independent of the angular momentum quantum number l, and restricting the summation over partial waves to $l\leq kR_{ch}$, we arrive at Eq. (7), Eq. (8), and Eq. (9), which correspond to the scattering (i.e., σ_{sc}), removal (i.e., σ_r), and total (i.e., σ_{tot}) cross sections, respectively. The parameters α and β are defined in Eq. (10). By carrying out the summation from l=0 to $l=kR_{ch,}$ Eq. (11) is derived. The channel radius is given by Eq. (12).

$$\sigma_{sc} = \pi(R_{ch}+\lambda)^2(1+\alpha^2-2\alpha\cos\beta) \tag{7}$$

$$\sigma_r = \sigma_{tot}-\sigma_{sc} = \pi(R_{ch}+\lambda)^2(1-\alpha^2) \tag{8}$$

$$\sigma_{tot} = \pi(R_{ch}+\lambda)^2(1-\alpha\cos\beta) \tag{9}$$

$$\begin{gathered}\alpha = \exp(-2\mathrm{Im}\delta_l) = \exp(-2\mathrm{Im}\delta)\\ \beta = 2\mathrm{Re}\delta_l = 2\mathrm{Re}\delta\end{gathered} \tag{10}$$

$$\sum_{l=0}^{kR_{ch}}(2l+1) = (kR_{ch}+1)^2 = (\lambda+R_{ch})^2k^2 \tag{11}$$

$$\begin{gathered}R_{ch} = r_0A^{\frac{1}{3}} + r_A\sqrt{E} + r_2\\ r_A = r_{10}\ln A + \frac{r_{11}}{\ln A}\\ r_0, r_{10}, r_{11}, r_2 = cte\end{gathered} \tag{12}$$

The optical potential describing the nuclear interaction between a neutron and a nucleus (i.e., n–N) is expressed as −V−iW, where V and W are both positive quantities, and the potential does not include any Coulomb interaction. The phase shift δ is calculated using the WKB approximation. Its real part represents a zeroth-order approximation (Mohr, 1957) for a square-well potential of radius R, given by (K−k)R, where K is the real part of the internal wave number K′, and k′=k since there is no external potential. Thus, the real wave numbers inside and outside the nucleus are defined by Eq. (13). The parameter β is determined by the real part of the potential (i.e., V), while the attenuation factor α is mainly governed by the imaginary component (i.e., W). Eq. (14) and Eq. (15) provide the expressions for α and β, respectively.

$$\begin{gathered}K^2 = \frac{2m(E+V)}{\hbar^2}\\ k^2 = \frac{2mE}{\hbar^2}\end{gathered} \tag{13}$$

$$\alpha = \exp\left(-\frac{\bar{R}}{\lambda}\right) = \exp\left(-\frac{2mW\bar{R}}{\hbar^2k}\right) \tag{14}$$

$$\beta = 2(K-k)R = \frac{2R\left(\sqrt{2m(E+V)}-\sqrt{2mE}\right)}{\hbar} \tag{15}$$

The parameter λ represents the mean free path of a neutron within the nucleus. The average chord length $\overline{R}$ traversed by a neutron as it passes through the nucleus is given by Eq. (16).

$$\overline{R} = \frac{\int_0^R 2\pi x I\sqrt{R^2-x^2}dx}{\int_0^R 2\pi x I dx} = \frac{4R}{3} \tag{16}$$

Where, I denotes the neutron flux, which represents the number of neutrons interacting per unit area. Given that the nuclear radius $R \propto A^{1/3}$, Eq. (17) provides the expression for the real part of the optical potential. The first term in this equation incorporates both the isoscalar and isovector components of the optical potential(Lane, 1962) (Satchler, 1983a) (Bhattacharya and Kailas, 1983) of the optical potential (Gould et al., 1986) (Anderson and Grimes, 1990), where Z is the atomic number of the target nucleus, while the second term describes its energy dependence.

$$\begin{gathered} V = V_A + V_E\sqrt{E} \\ V_A = V_0 + V_1\left(1-\frac{2Z}{A}\right) + \frac{V_2}{A} \\ V_0, V_1, V_2, V_E = cte \end{gathered} \tag{17}$$

The imaginary part of the potential is given by Eq. (18).

$$\begin{gathered} W = W_0 + W_E\sqrt{E+V} \\ W_0, W_E = cte \end{gathered} \tag{18}$$

The fitted global constants are:

Parameter	Value	Unit	Physical Role
V_0	46.51	MeV	Isoscalar depth
V_1	6.74	MeV	Isovector term
V_2	−117.52	MeV	Surface/mass correction
V-E	−3.22	MeV½	Energy dependence

The negative value of V-E reflects the known decrease of the real potential depth with increasing neutron energy.

Parameter	Value	Unit	Physical Role
W_0	5.293	MeV	Volume absorption
W_E	0.3388	MeV½	Energy-dependent absorption
α_0	0.2929	—	Attenuation constant

The positive value of W_E reflects the physical increase of absorption channels with increasing energy.

Parameter	Value	Unit
r_0	1.378	fm
r_{10}	−0.02298	fm
r_{11}	0.1027	fm
r_2	0.2322	fm

These values provide global fits to neutron total cross sections across a wide mass range

The total kinetic energy of a neutron within the nucleus, considering an attractive potential well of depth V, is given by E+V. Since the magnitude of the real part of the optical potential decreases with increasing neutron energy, while the imaginary part increases, this implies that the energy derivative of the real potential, V_E, is negative, and the energy derivative of the imaginary potential, W_E, is positive.

Even then, if we accept Peterson's assumption [20] of the neutron as a light ray, the average chord length inside the nucleus, considering beam bending away from the normal, would be less than our result of 4R/3 instead of greater than 4R/3 as obtained in the mentioned reference. However, these results converge to our result of 4R/3 for a refractive index equal to one, i.e., at energies higher than the real part of the nuclear potential, they yield a trivial agreement.

It can be said that, this approach revisits the Ramsauer model for neutron-nucleus scattering and presents a theoretically consistent framework that simplifies interpretation compared to traditional optical model calculations. While the optical model accounts for scattering with multiple partial waves, it lacks intuitive physical transparency. By assuming a constant complex phase shift δ across all partial waves, and summing up to a maximum angular momentum $L=kR_{ch}$, the model leads to compact analytical expressions for scattering, removal, and total cross sections. In addition, the approach applies the WKB approximation to derive the real and imaginary parts of the phase shift in terms of the optical potential parameters V and W. This enables analytical expressions for attenuation (i.e., α) and phase shift (i.e., β), where β governs the oscillatory behavior of the scattering amplitude and α characterizes absorption. Finally, a key point of this approach is a critique and replacement of the classical optics-based interpretation of phase shifts found in prior literature Peterson (1962). The authors highlight that treating neutrons as light rays yields physically inconsistent results, such as a refractive index less than one and unrealistic critical angles for transmission. In contrast, the WKB-based derivation presented here provides a robust quantum mechanical foundation for describing neutron interactions with a spherical nuclear potential. The model ultimately leads to intuitive physical parameters, including the mean free path, average chord length, and potential energy dependence. The derived expressions show convergence to asymptotic behavior at high energies and establish clearer links between phenomenological optical potential parameters and observed scattering phenomena.

The results of the given analytical method for cross section calculation for selected elements

To demonstrate the applicability of the Ramsauer model in the intermediate neutron-energy region, neutron cross-section data have been calculated for selected nuclei and compared with evaluated data from the ENDF library, as presented in **Table 1**. The chosen target nuclei - **C-12, O-16, Ag-107, and U-235** - were selected to represent a broad range of atomic masses and to reflect their practical significance in reactor physics and neutron shielding applications. To quantitatively evaluate the predictive accuracy of the analytical Ramsauer model, the **relative error**, defined by **Eq. (19)**, was computed by comparing the model's calculated cross sections with corresponding ENDF reference values over the selected neutron energy range of **0.25 to 2 MeV**.

Table 1: Comparison of Neutron Cross Sections from ENDF and Analytical Ramsauer Model across Multiple Energies for Selected Elements

Element	Cross section (barn)	ENDF/B-VIII.0					The anlytical approach				
		Energy (MeV)									
		0. 25	0.5	1	1.5	2	0. 25	0.5	1	1.5	2
C-12	σsc	3.96	3.39	2.6	2.05	1.70	3.29	1.91	1.26	1.08	1.01
	σtot	4	3.4	2.57	2.01	1.73	7.65	4.46	2.92	2.48	2.29
	σr	0.04	0.01	0.03	0.04	0.03	4.27	2.55	1.66	1.4	1.28
	σsc	7.40	6.22	4.86	2.87	3.11	8.27	5.68	3.86	3.03	2.57

Ag-107	σtot	7.78	7.26	6.41	5.75	5.22	16.74	11.51	7.82	6.15	5.22
	σr	0.38	1.04	1.55	2.88	2.11	8.46	5.83	3.96	3.12	2.65
O-16	σsc	3.37	4.41	8.12	2.01	1.57	4.77	2.60	1.46	1.09	0.94
	σtot	3.37	4.41	8.12	2.01	1.57	10.48	5.77	3.29	2.48	2.12
	σr	0	0	0	0	0	5.71	3.17	1.82	1.39	1.18
U-235	σsc	7.72	5.53	3.90	3.56	3.80	9.89	6.74	4.78	4.16	3.93
	σtot	10.22	8.39	6.85	6.83	7.25	19.86	13.53	9.60	8.35	7.89
	σr	2.5	2.86	2.95	4.26	3.45	9.97	6.77	4.82	4.19	3.96

$$\text{RelativeError}(\%)=\left|\frac{\sigma_{\text{analytical}}-\sigma_{\text{ENDF}}}{\sigma_{\text{ENDF}}}\right|\times 100 \tag{19}$$

To further illustrate the model performance, Figure. 1 and Figure. 2 present the total neutron cross section (σ_{tot}) as a function of energy for the studied nuclides, comparing the analytical Ramsauer predictions with ENDF/B-VIII.0 data. For all materials, the analytical model follows the overall decreasing trend of σ_{tot} with increasing neutron energy, which is the dominant behavior in the fast and epithermal range. However, the analytical values systematically overestimate the magnitude of σ_{tot}, particularly below 1 MeV, where compound-nucleus resonance effects contribute significantly to the evaluated data. This discrepancy reflects the simplified treatment of absorption through an energy-independent imaginary potential and the absence of explicit resonance modeling.

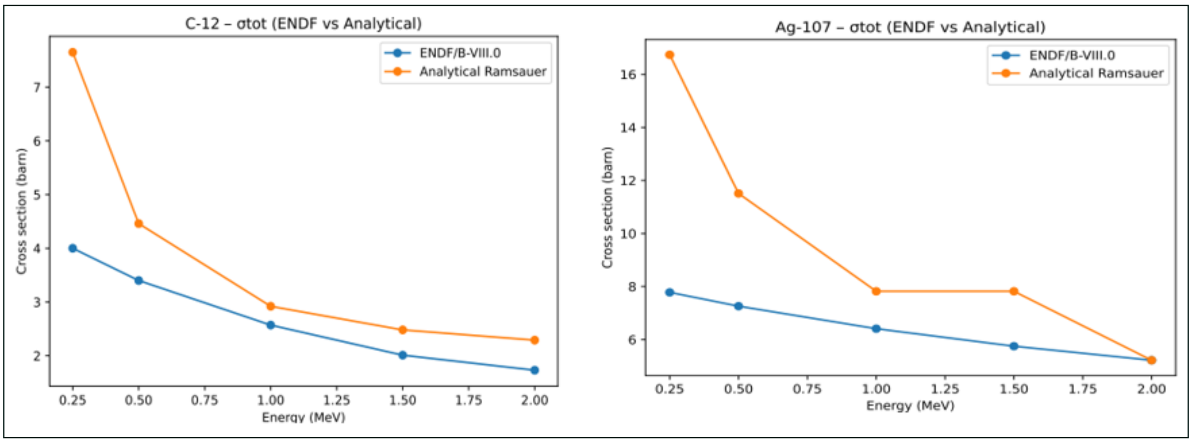

Figure 1: Total neutron cross section (σ_{tot}) as a function of energy for C-12 and O-16, comparing ENDF/B-VIII.0 data with the analytical Ramsauer model. The analytical model reproduces the overall fast-neutron energy trend but systematically overestimates σ_{tot}, particularly below 1 MeV.

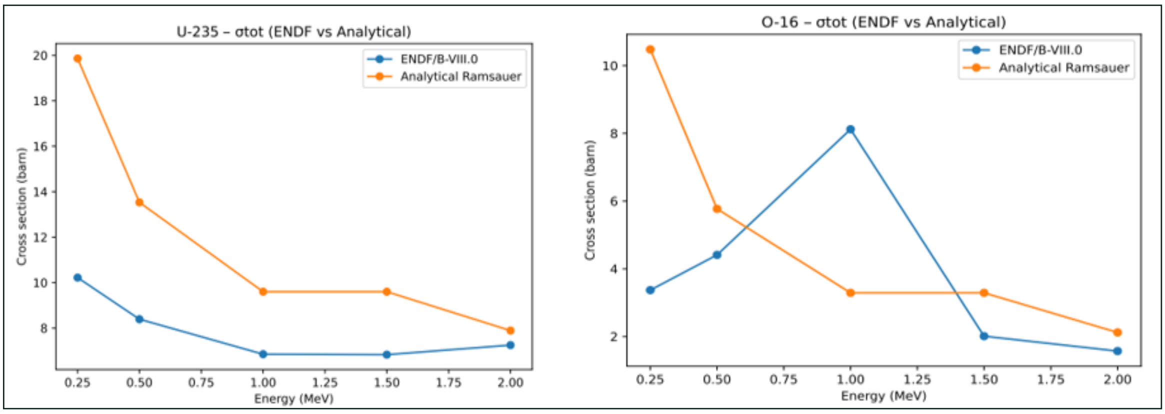

Figure 2: Total neutron cross section (σ_{tot}) for Ag-107 and U-235 in the 0.25–2 MeV range. While the analytical Ramsauer model preserves the qualitative energy dependence relevant to fast-reactor applications,

it overpredicts the magnitude of σ_{tot} due to simplified absorption modeling.

The analytical Ramsauer model reproduces the main fast-neutron behavior of the scattering cross section, showing a clear decrease of **σsc** with energy for all studied nuclides in **0.25–2 MeV**. The mean deviation from ENDF/B-VIII.0 is ~33% (best for **Ag-107 ≈15%**, largest for **O-16 ≈46%**), which is adequate for rapid scoping in fast/epithermal transport where overall trends matter more than fine resonances.

For materials relevant to fast reactors, the results are most useful when interpreted as a **trend/sensitivity tool**: **C-12** represents moderator/reflector behavior (spectrum shaping via scattering), **U-235 and O-16** represent fuel and fuel-matrix constituents affecting multiplication and leakage, and **Ag-107** is relevant to **control/absorber materials** where accurate removal matters. The model's smoother curves indicate it captures potential scattering, but it does not resolve compound-nucleus resonance structure; This behavior is clearly observed in the $\sigma_{tot}(E)$ plots shown in Fig. 1 and Fig. 2. For **U-235**, the qualitative energy trend of σr is preserved, but quantitative agreement still requires improved (energy-dependent) imaginary potential.

Overall, the method is best applied in fast-reactor and shielding workflows for **quick cross-section screening, spectrum-trend studies, and parametric comparisons** before running high-fidelity deterministic/Monte Carlo calculations.

Conclusion

This study has presented a theoretically consistent analytical formulation of the nuclear Ramsauer model for neutron–nucleus interactions in the intermediate-energy range (0.25–2 MeV). Starting from the optical potential framework and employing the WKB approximation, compact closed-form expressions were derived for the scattering (σ_sc), total (σ_tot), and reaction (σ_r) cross sections under the assumption of an angular-momentum-independent complex phase shift. The real and imaginary parts of the phase shift were explicitly related to the optical potential components, providing a transparent physical interpretation of attenuation and phase oscillation effects.

A central outcome of this work is that the model successfully reproduces the global energy dependence of the **scattering cross section**, σ_sc, across light to heavy nuclei. This result is particularly significant because, in the fast and epithermal energy ranges, neutron transport is predominantly governed by elastic and potential scattering. The scattering cross section controls spectrum shaping, neutron moderation in structural materials, leakage behavior, and flux redistribution in reactor systems. Therefore, capturing the correct trend and magnitude of σ_sc is physically more critical for intermediate-energy transport analysis than resolving fine resonance structures in absorption.

Benchmarking against ENDF/B-VIII.0 data for ^{12}C, ^{16}O, ^{107}Ag, and ^{235}U demonstrates that the model reproduces the decreasing trend of σ_sc with energy with mean deviations on the order of 15–45%, depending on mass region. Agreement improves for medium and heavy nuclei, consistent with the semiclassical assumptions underlying the WKB treatment. This indicates that the dominant potential-scattering mechanism is adequately captured within the simplified Ramsauer framework.

In contrast, the reaction cross section σ_r is systematically overestimated, particularly for light nuclei where evaluated data show negligible absorption in the considered energy range. This limitation arises from the simplified treatment of the imaginary optical potential as energy-independent, the absence of explicit compound-nucleus resonance modeling, and the l-independent phase-shift assumption, which enhances absorption uniformly across partial waves. Consequently, while the model preserves qualitative behavior for heavier nuclei such as ^{235}U, quantitative prediction of σ_r requires further refinement through energy-dependent or surface absorption terms.

The applicability of the WKB approximation, which formally requires kR≫1, was also assessed. At the lower end of the investigated energy range, this condition is only marginally satisfied for light nuclei, implying reduced accuracy near 0.25 MeV. The model's consistency improves with increasing energy and nuclear mass, where semiclassical assumptions are better fulfilled.

The primary contribution of this work lies in establishing a compact, internally consistent analytical connection between optical potential parameters and measurable cross sections, avoiding full numerical partial-wave solutions while preserving the essential physics of intermediate-energy scattering. Unlike classical refraction-based Ramsauer interpretations, the present derivation remains fully grounded in quantum mechanical optical-model theory and clarifies the physical meaning of the attenuation and phase parameters.

Overall, the model is best interpreted as a physically transparent trend-analysis tool, particularly valuable for studying scattering-dominated behavior in the fast/epithermal regime. It is not intended to replace evaluated nuclear data libraries or high-fidelity transport calculations for precision engineering design. Future improvements incorporating energy-dependent imaginary potentials and partial-wave corrections would enhance quantitative accuracy while maintaining analytical simplicity [21-28].

References

1. Hughes DJ (2016) Neutron cross sections. Elsevier.
2. Zohuri B (2019) Neutronic analysis for nuclear reactor systems. Springer.
3. Lane A, Thomas R (1958) R-matrix theory of nuclear reactions. Reviews of Modern Physics 30: 257.
4. Feshbach H (1958) Unified theory of nuclear reactions. Annals of Physics 5: 357-390.
5. Team MC (2003) MCNP–a general Monte Carlo N-particle transport code, version 5. Book MCNP-A General Monte Carlo N-Particle Transport Code Version 5.
6. Brown, F.B., 2009. A review of best practices for Monte Carlo criticality calculations.
7. Carlson AD, Pronyaev VG, Smith DL, Larson NM, Chen Z et al., (2009) International evaluation of neutron cross section standards. Nuclear Data Sheets 110: 3215-3324.
8. Abfalterer W, Bateman F, Dietrich F, Finlay R, Haight R, Morgan G (2001) Measurement of neutron total cross sections up to 560 MeV. Physical Review C 63: 044608.
9. Brown DA (2018) ENDF/B-VIII. 0: the 8th Major Release of the ENDF/B Library. Brookhaven National Lab.(BNL), Upton, NY (United States).
10. Shore F, Sailor V (1958) Slow Neutron Resonances in U 235. Physical Review 112: 191.
11. Satchler GR (1983b) Direct nuclear reactions.
12. Fesbach H (1992) Theoretical nuclear physics: nuclear reactions.
13. Koning A, Delaroche J (2003) Local and global nucleon optical models from 1 keV to 200 MeV. Nuclear Physics A 713: 231-310.
14. Hodgson PE (1994) The optical model of elastic scattering, The Nucleon Optical Model. World Scientific 19-39.
15. Grimes S, Anderson J, Bauer R, Madsen V (1998) Justification of a simple Ramsauer model for neutron total cross sections. Nuclear science and engineering 130: 340-347.
16. Lawson J (1953) A diffraction effect illustrating the transparency of nuclei to high energy neutrons. The London, Edinburgh, and Dublin Philosophical Magazine and Journal of Science 44: 102-103.
17. Angeli I, Csikai J (1970) Total neutron cross sections and the nuclear Ramsauer effect. Nuclear Physics A 158: 389-392.
18. Angeli I, Csikai J (1971) Total neutron cross sections and the nuclear Ramsauer effect:(II). En= 0.5–42 MeV. Nuclear Physics A 170: 577-583.
19. Angeli I, Csikai J, Nagy P (1974) Semiclassical description of fast-neutron cross sections. Nuclear Science and Engineering 55: 418-426.
20. Peterson J (1962) Neutron giant resonances—nuclear Ramsauer effect. Physical Review 125: 955.

21. Anderson J, Grimes S (1990) Nuclear Ramsauer effect and the isovector potential. Physical Review C 41: 2904.
22. Bhattacharya S, Kailas S (1983) The real part of the nucleon-nucleus optical potential. Zeitschrift für Physik A Atoms and Nuclei 309: 325-329.
23. Brown DA, Chadwick MB, Capote R, Kahler A, Herman M el al., (2018) ENDF/B-VIII. 0: the 8th major release of the nuclear reaction data library with CIELO-project cross sections, new standards and thermal scattering data. Nuclear Data Sheets 148: 1-142.
24. Gould C, HAASE D, SEAGONDOLLAR L, SODERSTRUM J, NASH K et al., (1986) Spin-Spin Potential in Npol 27Alpol and the Nuclear Ramsauer Effect. Phys. Rev. Lett. 53: 2371.
25. Lane A (1962) Isobaric spin dependence of the optical potential and quasi-elastic (p, n) reactions. Nuclear Physics 35: 676-685.
26. Mohr C (1957) The WKB method for a complex potential. Australian Journal of Physics 10: 110-117.
27. Mukhopadhyay T, Lahiri J, Basu D (2011) Theoretical estimates of cross sections for neutron–nucleus collisions. Annals of Nuclear Energy 38: 1452-1457.
28. Satchler G (1983a) Int. series of monographs on Physics. Oxford University Press, Direct Nuclear reactions.